SLAC – PUB – 4135
October 1986
(T/E)

# Recent Results on the Charm Sector*

RAFE H. SCHINDLER

*Stanford Linear Accelerator Center*
*Stanford University, Stanford, California, 94305*

## 1. INTRODUCTION

The understanding of charmed meson decays has progressed rapidly in recent years. In the first section of this chapter, a brief discussion of charm particle spectroscopy is presented reviewing the current status of the field. In the next section, the phenomenology of the weak decays of ground state charmed mesons is outlined and discussed in light of recent measurements of the meson total widths. A brief discussion of the phenomena of $D^0\bar{D}^0$ mixing is included. In the subsequent sections, the measurements of semileptonic and hadronic charm decays are summarized and discussed in light of the phenomenology, leading to the emergence of a coherent picture of the underlying physics and pointing towards some as yet unanswered experimental and theoretical questions.

*To be published in* **High Energy Electron-Positron Physics**
*World Scientific Publishing Company*

⋆ Work supported by the Department of Energy, under contracts DE-AC03-76SF00515.

## 2. THE CHARM SPECTROSCOPY

In the standard parton model, the light $u,d,$ and $s$ quarks are expected to combine with the heavier charmed $(c)$ quark to form the three lowest lying pseudoscalar states: $D^0$ $(c\bar{u})$, $D^+$ $(c\bar{d})$ and $D_s$ $(c\bar{s})$.[1] Spectroscopically, these correspond to the $^1S_0$ states. Unless otherwise stated, a specific state will always imply its charge conjugate as well. The $D^0$ and $D^+$ form an isotopic doublet; the $D_s$ an isosinglet. These states have been isolated in $e^+e^-$ annihilation, hadroproduction, photoproduction, and $\nu$-scattering experiments. The masses[2] and lifetimes[3] of the groundstates are summarized in Table I.

TABLE I. Ground and Excited States of Charmed Mesons[2][3][4]

| Charmed Meson | Quark Content | Mass $GeV/c^2$ | Width (MeV) (Lifetime $\times 10^{-13}$) | J$^P$ Assignment |
|---|---|---|---|---|
| $D^0$ | $c\bar{u}$ | $1864.6 \pm 0.6$ | $(4.43^{+0.19}_{-0.17})$ | $0^-$ |
| $D^+$ | $c\bar{d}$ | $1869.3 \pm 0.6$ | $(10.29^{+0.54}_{-0.43})$ | $0^-$ |
| $D_s^+$ | $c\bar{s}$ | $1970.5 \pm 2.5$ | $(3.85^{+0.65}_{-0.48})$ | $0^-$ |
| $D^{*0}$ | $c\bar{u}$ | $2007.2 \pm 2.1$ | $\leq 5.0$ | $1^-$ |
| $D^{*+}$ | $c\bar{d}$ | $2010.1 \pm 0.7$ | $\leq 2.2$ | $1^-$ |
| $D_s^{*+}$ | $c\bar{s}$ | $2110 \pm 6$ | - | $1^-$ |
| $D^{**0}$ | $c\bar{u}$ | $2420 \pm 6$ | $70 \pm 21$ | $1^+$,$2^+$ |

Each ground state meson is expected to have a vector state ($^3S_1$)corresponding to the parallel alignment of its constituent quark spins. The $D^{*0}$ and $D^{*+}$ are now well established.[5] The excited state of the $D_s$ has only recently been established in $e^+e^-$ annihilation,[6] [7] through both its direct decay, and its associated production ($e^+e^- \rightarrow D_s\bar{D}_s{}^*$) near threshold.

As in the spectrosopy of light quark mesons, a set of orbitally excited charmed mesons is also expected with the lowest lying states having spectroscopic and quantum number assignments: $^1$P$_1$ ($1^+$) or $^3$P$_j$ ($0^+$, $1^+$ and $2^+$), and masses typically 500 MeV/c$^2$ higher than the ground states.[8]

Figure 1 shows a typical set of mass splittings expected for bound $c\bar{q}$ states in both nonrelativistic and relativistic potential models. The first candidate for an orbitally excited state ($D^{**0}$ ) has only recently been observed.[9] Figure 2 shows the experimental evidence for the state.

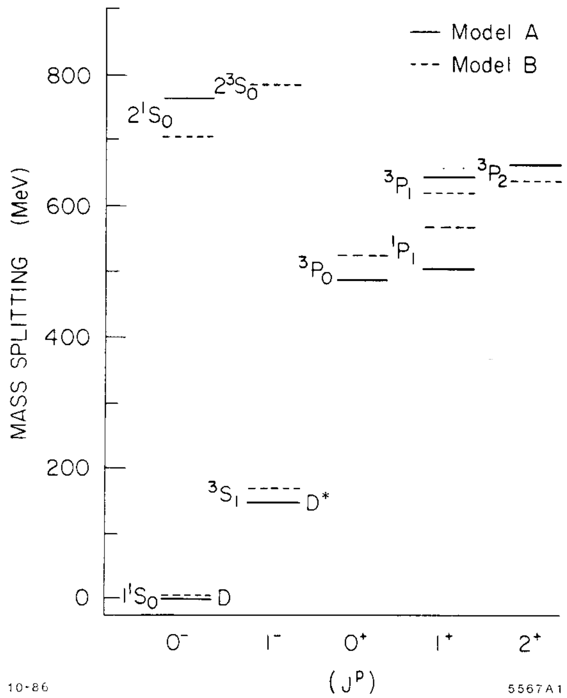


Fig. 1. Expected states for $D$ and $D_s$ mesons. Model A from Eichten *et al.*, Model B from Godfrey and Isgur ref.[8].

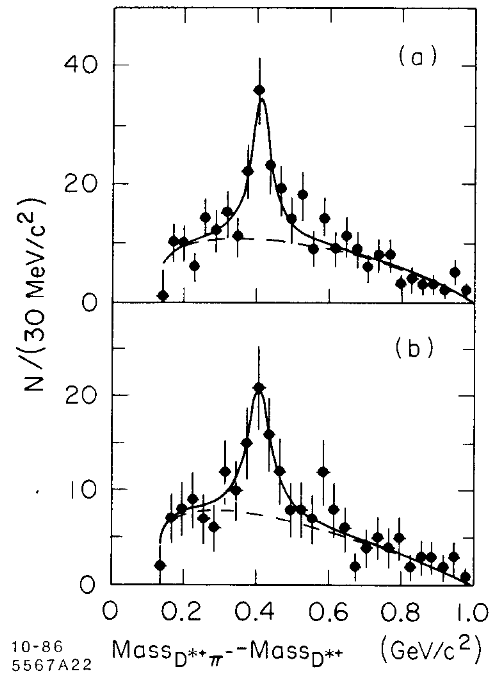


Fig. 2. $D^{**0}$ candidate from Albrecht *et al.*, ref.[9].

The $D^o$, $D^+$ and $D_s$, being the lightest charmed mesons, must decay weakly through a charm-changing charged current. The details of these decays will encompass the greater part of the chapter. The vector states $D^{*0}$ and $D^{*+}$ decay strongly and electromagnetically to the ground states through $\pi^{\pm}$, $\pi^0$ and $\gamma$ emission. Some of these transitions (such as $D^{*0} \to \pi^- D^+$) are energetically forbidden (see Figure 3). While all the decays have been measured, there are still discrepancies in the branching fractions, owing to the difficulty of the measurements. The charm-strange $D_s^{*+}$, being an isosinglet, cannot decay strongly to the $D_s^+$ via $\pi^0$ emission. The $\gamma$ transition is uninhibited, and is expected to dominate the $D_s^{*+}$ decay. The world average for the mass difference between the $D_s^+$ and $D_s^{*+}$ is now measured to be $132 \pm 5 \pm 4$ MeV/c$^2$, forbidding an isospinviolating decay through $\pi$ emmission. The difference in squared masses between vector and pseudoscalar states for both the $D$ and the $D_s$ lie close to the constant found for all lighter mesons (see Table II) to be expected if the meson wavefunction at the origin is determined by the long range confining part of the potential.[11]

TABLE II. Difference in $(\mathrm{Mass})^2$ for Pseudoscalar and Vector Mesons.[10]

| Mesons | $(\mathrm{Mass})^2$ Difference |
|---|---|
| $\rho - \pi$ | 0.574 |
| $K^* - K$ | 0.556 |
| $D^* - D$ | 0.546 |
| $D_s^* - D_s$ | $0.55 \pm 0.01$ |
| $B^* - B$ | $0.55 \pm 0.05$ |

The lowest-lying orbitally excited states are at sufficiently high masses to allow the possibility of strong $\pi$ decays to both the ground states and the vector states from the $^1P_1$, $^3P_1$, and $^3P_2$ states. Parity conservation in the strong decay allows the $^3P_0$ to decay only to the ground state, through single $\pi$ emission. Widths of 50 to 100 MeV/c$^2$ are expected for all these decays, making it difficult to distinguish the multiplet of states whose mass splitting should be comparable. Mixing between the singlet and triplet J=1 states may further complicate the picture. Multipion and other strong decays are also likely to occur for these states when energetically allowed. At present, the only candidate for one or more of these $1^+$ or $2^+$ states is the 70 MeV/c$^2$ wide resonance $D^{**0}(2420)$, which is observed to

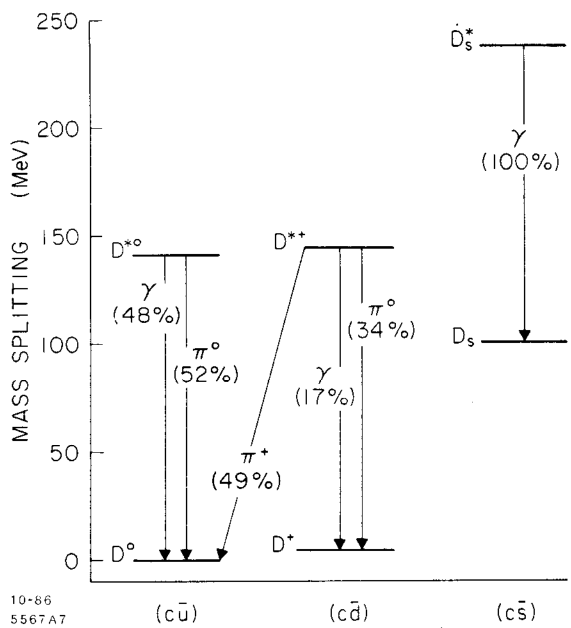


Fig. 3. Decays of $D^{*+}$ and $D^{*0}$.

decay to $D^{*+}\pi^-$.[9] This state appears to play a significant role in charm fragmentation at high energies.

## 3. PHENOMENOLOGY OF CHARMED MESON DECAYS

The weak decays of the charmed mesons can most naively be thought of as the beta decay of a free charmed quark. The partial width associated with such a process (pictured in Figure 4) is given by:

$$\Gamma_0(c \to s\ u\ \bar{d}) = \frac{G_F^2 M_c^5}{192\pi^3} \tag{1}$$

Here, the light quark is ignored, as is the phase space correction ($\sim 1/2$) for the $s$-quark mass. There are five such processes shown in Figure 4; two are Cabibbo-allowed semileptonic, and three are Cabibbo-allowed nonleptonic corresponding to three possible colors. In total the width in (1) must be multiplied by five (if the Cabibbo angle is ignored). That is, $\Gamma^{tot} = \Gamma^{NL} + \Gamma^{SL}$:

$$\Gamma^{NL} = 3 \times \Gamma_0 \qquad \Gamma^{SL} = 2 \times \Gamma_0$$

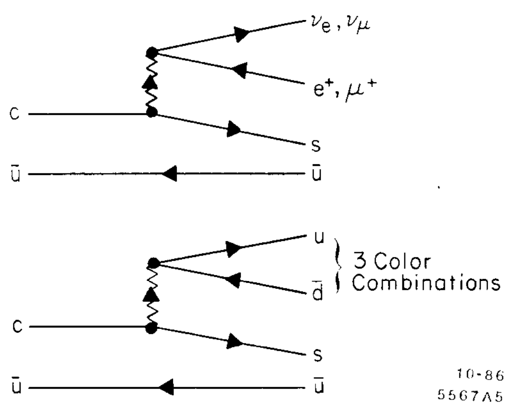

Fig. 4. The beta decay of the charmed quark.

The corresponding lifetime for a charmed quark mass ($M_c$) of 1.5 GeV/c$^2$ is about $6 \times 10^{-13}$ seconds. This naive model is commonly referred to as the spectator picture, since the light quark acts as a spectator in the decay, and plays no role. In this picture, the $D^0$ and $D^+$ and $D_s$ have equal lifetimes and semielectronic (or semimuonic) branching ratios of 20%.

### 3.1 Corrections to the Spectator Picture

The hadronic weak decays however are expected to be modified by strong interactions among the quarks that are not present in the semileptonic decays. The bare four-fermion point interaction is altered in lowest order by one loop hard gluon exchanges. The strong interaction effects are neatly accommodated in the Wilson coefficients ($c_\pm(q^2)$) in an effective weak Hamiltonian for the nonleptonic interaction:[12]

$$H^{NL}_{weak} = \frac{G_F}{\sqrt(2)} (V^*_{cs}V_{ud})(c_+O_+ + c_-O_-)$$
$$\text{where} \quad O_\pm = 1/2\left[(\bar{u}d)(\bar{s}c) \pm (\bar{s}d)(\bar{u}c)\right]$$

and $(\bar{q}_1 q_2)$ implies the usual V-A current $(\bar{q}_1\gamma^\lambda(1-\gamma^5)q_2)$. The term $O_-$ $(O_+)$ transforms like an SU(4) 20-plet (84-plet). In the charm-changing piece, these contain respectively the SU(3) 6-plet and 15-plet. The coefficients (at fixed $q^2$) are related in leading log and next-to-leading log approximation by, $c_- = 1/\sqrt(c^+)$, implying that only one independent parameter governs $H^{NL}_{weak}$. The coefficients $c_\pm$ are unity at $q^2 = \infty$, corresponding to the property of the strong interactions of asymptotic freedom. The Hamiltonian then reverts back to that of *free quarks*. For values of $q^2$ corresponding to the charmed quark mass $M_c \approx 1.5$ GeV/c$^2$, the value of $c_- \approx 2.0$ and $c_+ \approx 0.7$. The calculation of $c_\pm$ has been done to next order, and is found to reinforce the leading log calculation in direction but to be decreasing in magnitude[13] (see Figure 5).

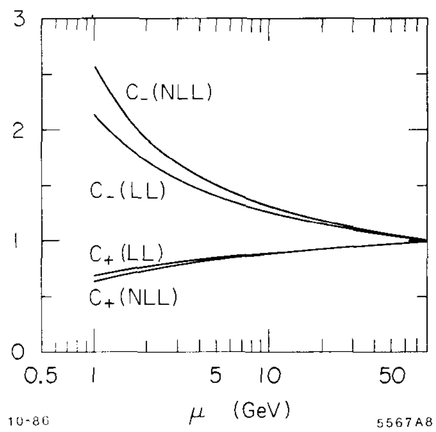


Fig. 5. Leading log and next to leading log values for $c_-$ and $c_+$.

The effect of the strong interaction is thus to *enhance* the sextet part of the charm-changing nonleptonic Hamiltonian, in analogy to *octet-enhancement* in the decays of strange mesons. The total nonleptonic width for charmed quark decay is thus increased:

$$\Gamma^{NL} = \left[\frac{2c_+^2 + c_-^2}{3}\right] \times [3\Gamma_0]$$

The semileptonic branching ratio ($B_l$) is correspondingly reduced to:

$$B_l = \frac{\Gamma(c \to eX)}{\Gamma(c \to all)} = \left[\frac{1}{2_{SL} \;+\; (2c_+^2 + c_-^2)_{NL}}\right] \tag{2}$$

For the values of $c_\pm$ evaluated at $M_c \approx 1.5$ GeV/c$^2$, the semileptonic branching ratio, $B_l \approx 14\%$. This is still an approximate calculation because of the uncertainty in the value of $q^2$ at which to evaluate the coefficients, the strength of still higher order corrections, and the effects of finite quark masses (which reduce the nonleptonic enhancement - see ref.[12]). Non-perturbative (soft-gluon) effects may also play a role,[14] and lead to additional non-leptonic enhancement. The best measurements at present for semileptonic decays are summarized in Table III.

TABLE III.

Semielectronic Branching Ratios[15]

| Meson | $B_l(\%)$ |
|---|---|
| $D^0$ | $7.5 \pm 1.1 \pm 0.4$ |
| $D^+$ | $17.0 \pm 1.9 \pm 0.7$ |
| $D_s$ | unmeasured |

As can be seen, the semileptonic branching fractions for the $D^0$ and $D^+$ are markedly different and straddle the prediction of the spectator model. The ratio of $D^0$ and $D^+$ semileptonic decays using tagged $D\bar{D}$ at the $\psi(3770)$ provided the first precise evidence that the $D^0$ and $D^+$ had different lifetimes.[15][16] The lifetime ratio and the semileptonic branching ratios are related as follows:

$$\frac{\tau(D^+)}{\tau(D^0)} = \frac{B_l(D^+)}{B_l(D^0)} = \frac{\Gamma(D^+ \to eX)/\Gamma(D^+ \to all)}{\Gamma(D^0 \to eX)/\Gamma(D^0 \to all)} = \frac{1/\Gamma(D^+ \to all)}{1/\Gamma(D^0 \to all)} \tag{3}$$

The equalities hold true assuming isospin invariance, and the smallness of Cabibbo-suppressed decays. The values in Table III yield $\frac{\tau(D^+)}{\tau(D^0)} = 2.3^{+0.5+0.1}_{-0.4-0.1}$.

This is nearly equal to the value $2.25^{+0.15}_{-0.14}$, obtained from subsequent direct lifetime measurements (see Table I). The closeness of these values suggests that the assumptions used in obtaining (3) are adequate, and no new physics need be invoked.

### 3.2 Beyond the Spectator Picture

The QCD-corrected spectator picture cannot accommodate the differences in the measured lifetimes for the $D^0$, $D^+$ and $D_s$, (see Table I) or the semileptonic branching ratios for the $D^0$ and $D^+$ (see Table III). It is difficult to draw conclusions from the lifetimes themselves because they depend on $M_c^5$, an unknown and rapidly varying quantity. The semileptonic branching ratio depends solely on the degree of non-leptonic enhancement. If the theoretical scale of non-leptonic enhancement is correct then *neither* the $D^0$ *nor* the $D^+$ decays like the spectator model predicts. The semileptonic decays then suggest the need for *both* a mechanism to enhance the $D^0$ width, and a mechanism to diminish the $D^+$ width. If the theoretical scale is incorrect to the extent that *either* the $D^0$ *or* the $D^+$ is spectator-like, then only one such additional mechanism would be necessary. To the extent that the pure leptonic decay of the $D_s$ ($D_s \to \tau^+\nu$) is not large, one might interpret the similarity in $D^0$ and $D_s$ lifetimes, as suggesting that they both undergo approximately the same level of non-leptonic enhancement.

3.2.1 <u>Non-spectator graphs and flavor annihilation.</u> The most direct way to enhance the $D^0$ or $D_s$ is to add additional diagrams denoted as W-exchange and W-annihilation, respectively (see Figure 6).[17] The W-annihilation graph is also present for Cabibbo-suppressed $D^+$ decays. These graphs have historically been ignored because at the quark level they are helicity suppressed ($\propto \frac{M_q^2}{M_c^2}$) and require a large wavefunction overlap of initial state quarks ($\propto \frac{f_D^2}{M_c^2}$ or $\propto \frac{f_{D_s}^2}{M_c^2}$). It has been argued that the helicity suppression may be removed by the presence of gluons in the meson

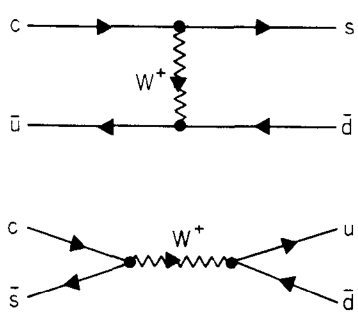

Fig. 6. W-exchange and W-annihilation graphs.

wavefunction,[18] or by the radiation of gluons from the light quark vertex.[19] The former is a largely non-perturbative effect, the latter, perturbative. This leaves the wavefunction overlap factor which is expected to be small owing to the small values ($\sim$ 150 MeV/c) of $f_D$ and $f_{D_s}$.[20] Recent work[21] suggests that a dynamical mechanism such as the presence of a resonance with quantum numbers equal to that of a $\bar{K}$ and mass close to the $D^o$, could also enhance the annihilation contribution.

Experimentally, certain decays of the $D^o$, such as $D^0 \rightarrow \bar{K}^0\phi, \bar{K}^0K^0$, and $\bar{K}^0K^{*0}$, should be clear signatures for W-exchange.[22] Here, the $\bar{u}$ quark of the initial state is absent in the final state meson. For the $D_s$ meson, final states with no net strangeness and no $s\bar{s}$ content (such as $\rho\pi$), would be characteristic of W-annihilation. Recent work[23] [24] however has suggested that rescattering effects, or non-planar diagrams (see Figure 7) may lead to final states that mimic the non-spectator decays. Flavor annihilation $\bar{u} \rightarrow \bar{d}$ occurs through the strong interaction, rather than the weak one. The situation will remain unresolved until there is a substantial increase in the world data.[25] [26]

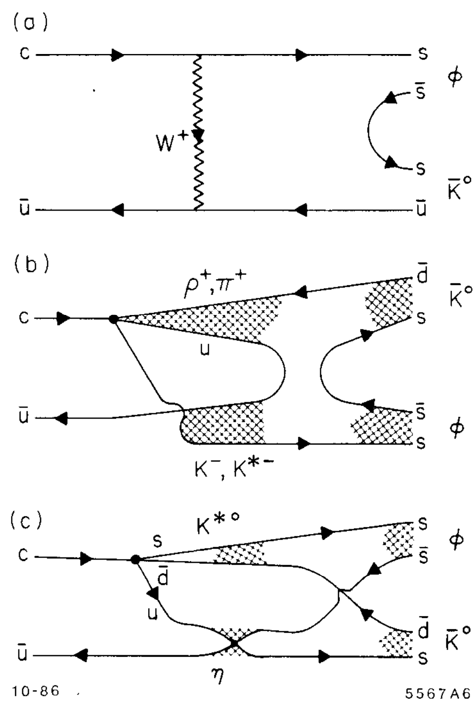


Fig. 7. (a) W-exchange leading to $\bar{K}^0\phi$, and (b)-(c) Non-planar diagrams simulating the same $D^o$ W-exchange final state.

3.2.2 Interference. The $D^+$ can receive enhancement in its Cabibbo-suppressed decays through W-annihilation diagrams. More importantly, the leading $D^+$ Cabibbo-allowed decays may be suppressed by cancellation of final state amplitudes in the presence of strong *color clustering* and QCD sextet enhancement.[27] Figure 8 indicates how color clustering leads to identical final state amplitudes which interfere in the $D^+$ due to the relative minus sign. To the extent that the coefficient $c_- >> c_+$, a cancellation can occur for pseudoscalar-pseudoscalar decays, while pseudoscalar-vector decays may be enhanced.[28]

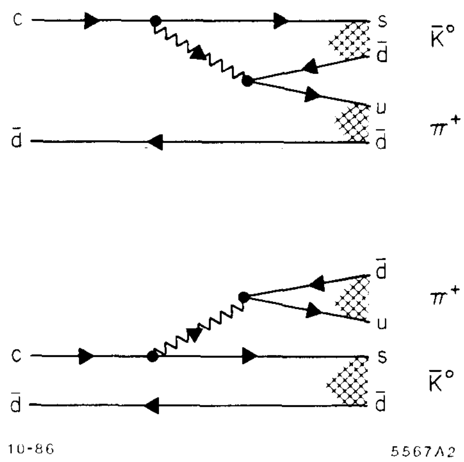


Fig. 8. Color clustered terms of the $O_-$ operator showing identical final states leading to interference.

The interference can also arise at the quark level, before hadronization, from the presence of two identical $\bar{d}$ quarks in the final state. The $D^+$ width then receives an extra term:[29]

$$\Gamma^{int}(D^+) = -(c_-^2 - 2c_+^2)\frac{12\pi^2}{{M_D}^2} f_D^2 \Gamma_0 \tag{4}$$

This term is negative for $c_- >> c_+$. More detailed calculations (e.g. potential and bag models) show that the effect of interference ranges from a few percent to as large as $\approx 50\%$ and may thus account for much of the $D^0$ and $D^+$ lifetime difference.[30]

3.2.3 Exclusive decays. The formalism of the effective weak Hamiltonian has been used to estimate the exclusive decay widths for charmed mesons.[31] To evaluate the transition matrix element for the desired decay the initial and final meson states are represented by their quark content. The matrix element of $H_{NL}$ is then evaluated by vacuum insertion and Fierz transformation (see ref.[31]). One expects that at least for energetic two-body decays, such a technique would be valid. Again, only one independent parameter ($c_-(q^2)$) is left assuming that $c_+$ is given by $1/\sqrt(c_-)$ to leading order. One of the most striking predictions of this analysis is the suppression of *color mismatched* decays. Figure 9 shows an example of how in the spectator picture, one expects $\Gamma(D^0 \to \bar{K}^0\pi^0)$ to be reduced by a factor of 1/2 compared to $\Gamma(D^0 \to K^-\pi^+)$ from isospin, and another factor of $(1/3)^2$ for the color mismatch. The combined factor of 1/18 is *further* reduced to about 1/40 when the QCD enhancement factors are applied. Similar suppressions are expected for decays like $D^0 \to \bar{K}^{*0}\pi^0$, $D^+ \to \phi\pi^+$, and $D_s \to \bar{K}^0K^+$. Each of these decays has analogous W-exchange or W-annihilation graphs as well.

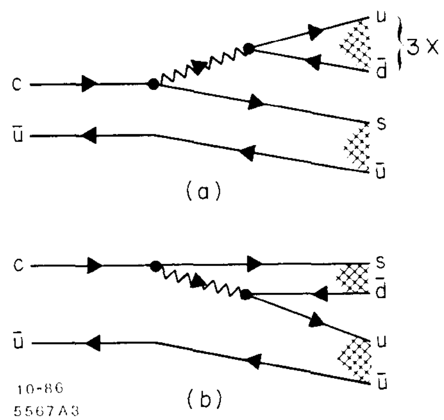


Fig. 9. (a) Color mismatched decay, and (b) Color allowed decay.

Recent work[24] [32] suggests however that the strength of these color cancellations should be moderated by an additional (second) free parameter $\xi$ (the *color screening* factor). A surprisingly good fit can then be obtained to many exclusive decays (see the following sections), with two free parameters, after accounting for form factors and final state interactions wherever possible. The parametization does not require the presence of W-exchange or W-annihilation, but does reproduce the strong interference effect for $D^+$ decays. The factor $\xi$ is found to be close to zero, and the remaining parameter ($c_-$) close to the nominal QCD value. The results are interpreted[33] in the formalism of the 1/N expansion (where N is the number of colors), and N$\to \infty$ in evaluating the matrix elements. For N=3, the earlier[31] color suppression result is recovered. Taking $\xi \approx 0$ *further* increases nonleptonic enhancement, yielding an estimate for $B_l(D^0)$:[33] [34]

$$B_l(D^0) = \frac{1}{2 + \frac{3}{2}(c_+^2 + c_-^2) + \frac{3\xi}{2}(c_+^2 - c_-^2)} \tag{5}$$

Using the nominal values of $c_\pm(q^2)$ and $\xi = 0$ a value of $\sim$ 11.5% is obtained for $B_l$, in better agreement with the data than what is obtained using $\xi = \frac{1}{3}$ (for N=3 colors) and the expression in (2) for $B_l$. This suggests the need for only a *small* additional contribution from a source such as W-exchange to reduce $B_l$ to $\sim$ 7.5%, the measured value. For the $D^+$, a term allowing for coherent interference of the $\bar{d}$ quarks, (as in (4)) is added to the denominator in (5), reducing the $D^+$ width and increasing $B_l(D^+)$.

A clearer understanding of the nonleptonic enhancement and suppression factors will only come about with more precise measurements of the $D$ meson system, and further measurements of the $D_s$ meson system. The latter, having the W-annihilation graph at the Cabibbo-allowed level, should provide a better means of determining the non-spectator contribution to charm decay. The complete pattern of hadronic and semileptonic $D_s$ decays would help determine the relative importance of individual decay mechanisms to all charmed hadrons.

3.2.4 $D^0\bar{D}^0$ mixing. Just as in the neutral kaon system, one considers the two strong interaction eigenstates ($D^0$ and $\bar{D}^0$) as linear combinations of two (approximate) CP eigenstates (denoted $D_1$ and $D_2$). Mixing of the states can occur either through finite differences in the masses or in the widths ($\Delta m = |m_1 - m_2|$, $\Delta\Gamma = |\Gamma_1 - \Gamma_2|$ ) of the CP eigenstates. Assuming CP invariance, these three quantities are all simaltaneous quantum numbers of $D_1$ and $D_2$. The usual parameters $x$ and $y$ are defined:

$$x = \frac{\Delta m}{\Gamma} \qquad\qquad y = \frac{\Delta\Gamma}{2\Gamma}$$

The mixing parameter $r$ is defined for $D^0$ decaying into the final state f:

$$r = \frac{Br(D^0 \to \bar{f})}{Br(D^0 \to f)} = \frac{x^2 + y^2}{2 + x^2 - y^2}$$

Here, r=0 for no mixing and r=1 for maximal mixing. Large mixing is expected when $\Delta m > \Gamma$, or $\Delta\Gamma \sim \Gamma$, the former being *real* transitions, while the latter come from oscillations induced by the large lifetime differences of the states (as is the case for $K^0\bar{K}^0$ mixing).

Naively, given the mass of the $D^0$ meson, and the abundance of allowed final states, one expects that differences associated with the widths ($\Delta\Gamma$) to be small, and any mixing should arise largely from the $\Delta m$ term. For charmed mesons, the $\Delta m$ term is induced by second order weak interactions embodied in the so called box diagrams (see Figure 10). The box-term is however small:

$$\Delta m \propto (M_s^2 - M_d^2) sin^2(\theta_c) f_D^2$$

Precise calculations yield values of $r \approx 10^{-7}$. Interest has been revived however by more recent calculations that suggest that long range effects (intermediate meson states) in the presence of SU(3)-breaking[35] may induce values of $r \leq$ (2 or 3) $\times 10^{-3}$ placing mixing close to the current regime of experimental sensitivity.

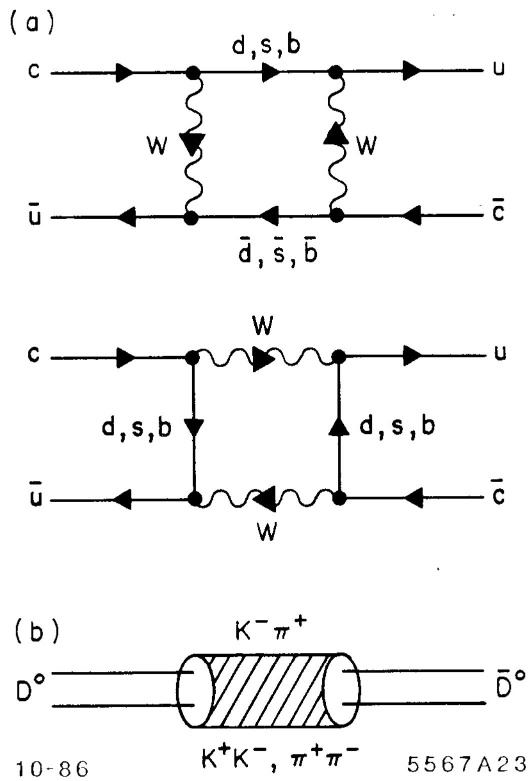


Fig. 10. (a) Box diagrams producing $D^0\bar{D}^0$ mixing, and (b) diagram depicting intermediate meson effects.

## 4. EXPERIMENTAL RESULTS

In the previous section, the phenomenology of the weak hadronic decays was elucidated, with tests at the *inclusive* level using the semileptonic decays alone to measure nonleptonic widths. In this section, experimental data on *exclusive* charmed meson decays is presented, and tied to the predictions of the last section.

## 4.1 The Semileptonic Decays

While abundant data on $D^0$ and $D^+$ semileptonic decays now exists, no data is currently available on the semileptonic decays of the $D_s$ . Interestingly, the pure leptonic decay of the $D_s$ may be as large as a few percent, being Cabibbo-allowed and phase-space favored. Should it be larger than anticipated due to an unexpectedly large value of the decay constant ($f_{D_s}$), it may complicate the understanding of the semileptonic decays of the $D_s$, and lead to confusion in our understanding of the magnitude of nonleptonic enhancement in $D_s$ decay.

We begin with a more detailed summary of the $D^0$ and $D^+$ semileptonic decay measurements. At the high energy $e^+e^-$ machines, the average value of $B_l \approx 12\%$ for the charmed hadron has been obtained through inclusive fragmentation studies.[38] Since this represents an unknown admixture of charmed hadrons, little can be learned. At the $\psi(3770)$, D mesons are produced in $D^0\bar{D}^0$ and $D^+D^-$ pairs in their phase space-ratio (55:45). It is thus possible to compute a precise average of both states, obtaining $11.0 \pm 1.1\%$.[38] At the $\psi(3770)$ it is also possible to enumerate the exclusive semileptonic decay channels. Events containing a $D\bar{D}$ pair where one D decays hadronically and the other one semileptonically, can be kinematically fitted with a single missing neutrino. This reconstruction technique is often referred to as *tagging*. At higher energies, *tagging* usually does not imply the full exclusive reconstruction of an event. The results are summarized in Table IV.[39]

TABLE IV.

Exclusive Semielectronic Branching Ratios[39]

| Exclusive Mode | $Br(\%)$ |
|---|---|
| $D^0 \to K^- e^+ \nu_e$ | $4.0 \pm 0.5 \pm 0.6$ |
| $D^0 \to K^- \pi^0 e^+ \nu_e$ | $1.3 \pm 0.5 \pm 0.2$ |
| $D^0 \to \bar{K}^0 \pi^- e^+ \nu_e$ | $2.6 \pm 0.9 \pm 0.4$ |
| $D^+ \to \bar{K}^0 e^+ \nu_e$ | $7.2 \pm 1.9 \pm 0.9$ |
| $D^+ \to K^- \pi^+ e^+ \nu_e$ | $3.9 \pm 0.8 \pm 0.7$ |

Isospin conservation allows extraction of $B(D^0 \to [K\pi]^- e^+ \nu_e) = 3.9 \pm 1.0 \pm 0.4$ and $B(D^+ \to [K\pi]^0 e^+ \nu_e) = 5.9 \pm 1.2 \pm 1.1$, independent of the nature of the $[K\pi]$ system. Figure 11 shows preliminary results for the $K\pi$ invariant mass in $D_{e4}$ decays indicating that while a large contribution appears to be $K^*(892)$, about $45 \pm 14\%$ may be nonresonant.[7] Hence only about *one fourth* of all semileptonic decays are nonresonant multibody decays. A similar pattern might be expected in the weak hadronic decays.

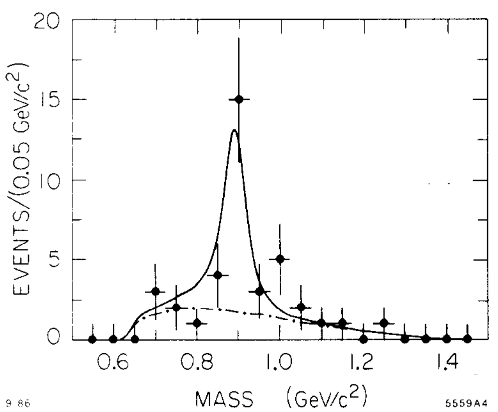


Fig. 11. Invariant mass for $K\pi$ system in $D^0$ and $D^+$ semileptonic decays.[7]

Summing the exclusive decays yields $7.9 \pm 1.1 \pm 0.7\%$ for $D^0$ and $13.1 \pm 2.2 \pm 1.4\%$ for $D^+$. These can be compared to the inclusive measurements of Table III, which contain the Cabibbo-suppressed semileptonic decays as well. The small difference suggests that such suppressed decays are consistent with the expectation of the Standard Model, namely that they be near to $tan^2(\theta_c) \approx .055$ in relative magnitude.

The isolation of semileptonic decays by *tagging* at the $\psi(3770)$ also makes it possible to measure the vector form factor $f_+(t)$ (where t is the momentum transfer of the kaon in $D_{e3}$ decay frame) thus probing the dynamics of the weak decay. The energy spectrum W(E$_K$) of the kaon in the decay frame of the D can be written wholly in terms of the momentum transfer (t), when the lepton coordinates are integrated out:

$$W(E_K) = |f_+(t)|^2 \, [E_K^2 - M_K^2]^{\frac{3}{2}}$$

$$\text{where} \qquad t = M_D^2 + M_K^2 - 2M_D \, E_K$$

The form factor is most directly parameterized as a simple pole, corresponding to the exchange of a virtual vector particle having quantum numbers of charm and strangeness (eg: the $D_s^{*+}$ ):

$$f_+(t) = f_+(0)\frac{M^2_{D_s^*}}{M^2_{D_s^*} - t} \qquad (6)$$

Figure 12 shows a fit to the kaon energy spectrum, with the simple pole form given by (6).[39] $W(E_K)$ is directly measurable since in tagged events it is possible to boost to the D decay frame *uniquely*, without the classic quadratic ambiguity. The pole mass is found to be $M_{D_s^*} = 2.1^{+1.7}_{-0.4}$ GeV/c$^2$ in excellent agreement with the value in Table I.

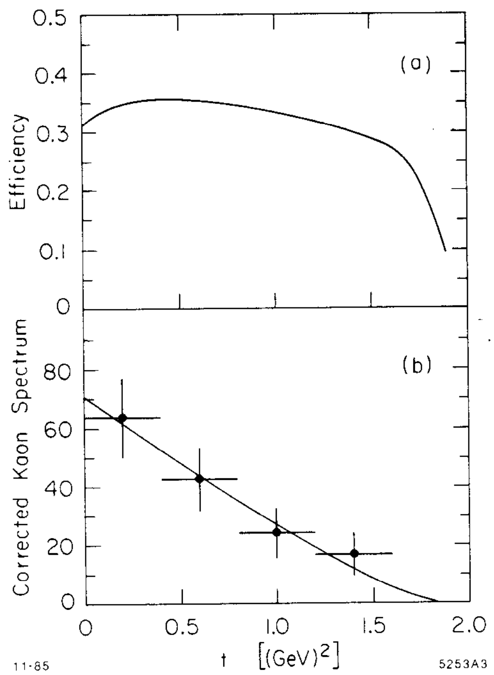


Fig. 12. (a) K detection efficiency in $D_{e3}$ decays, and (b) A fit for $f_+(t)$ to $W(E_K)$ assuming a simple pole form for the form factor.[39]

At present, no direct measurement of the Cabibbo-suppressed semileptonic decays has been made. These decays, when compared to the allowed decays of Table IV, would yield directly a value for $\frac{V_{cd}}{V_{cs}}$ the Kobayashi-Maskawa (K-M) matrix elements. It has been remarked that a similar comparison employing hadronic decays such as $D^+ \to \pi^+\pi^0$ with $D^+ \to \bar{K}^0\pi^+$, could provide a measurement of the K-M parameters.[40] More recent work[26] suggests however that SU(3) violations may still play a significant role, thus hindering the extraction of the K-M elements from such hadronic decays. The current values for the K-M parameters are $|V_{cd}| = 0.23 \pm 0.03$ and $|V_{cs}| \geq 0.66$. The former is obtained from neutrino production of charm,[41] and the latter from the exclusive decays of Table III and the form factor just described.[42]

### 4.2 Pure Leptonic Decays

The final topic in the leptonic sector is the purely leptonic decays of the $D^+$ and $D_s$ . These decays are expected at rates given by:

$$\Gamma_{D^+\to\mu^+\nu} = \frac{1}{8\pi} G_F{}^2 f_D{}^2 m_D m_\mu^2 |\, V_{cd}\, |^2 (1. - (m_\mu/m_D)^2)^2$$
$$\Gamma_{D_s^+\to\mu^+\nu} = \frac{1}{8\pi} G_F{}^2 f_{D_s}{}^2 m_{D_s} m_\mu^2 |\, V_{cs}\, |^2 (1. - (m_\mu/m_{D_s})^2)^2$$

For the $D^+$, given a lifetime of $10^{-12}$ seconds, a branching ratio of about 0.0002 is expected for values of $f_D$ of 150 MeV/$c^2$. For the $D_s$, given a lifetime of $3 \times 10^{-13}$ and $f_{D_s}$ of 150 MeV/c$^2$, the branching ratio is 0.0012. The $\tau$ decay modes however have branching ratios of 0.0004 and 0.011 respectively. Experimentally, these decays would be more difficult to observe since the three-body final states produce a softer muon spectrum. Of these four branching ratios, only a stringent limit for $D^+ \rightarrow \mu^+\nu$ of $\leq 8.4 \times 10^{-4}$ at 90% C.L. has been set.[7] This can be turned around to calculate a limit of 340 MeV/c at 90% C.L. on $f_D$ (see Figure 13). This limit rules out the perturbative radiative mechanism[19] proposed to overcome the helicity suppression of the W-exchange diagram for the $D^0$ .

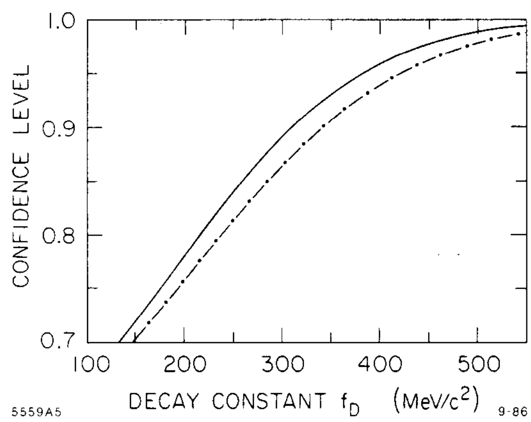


Fig. 13. A limit on the pure leptonic decay $D^+ \rightarrow \mu\nu$ in terms of the D meson decay constant $f_D$.[7]

### 4.3 Hadronic Decays

A large fraction of the Cabibbo-allowed and Cabibbo-suppressed decays of $D^0$ and $D^+$ are now measured, allowing for the first time a detailed study of the systematics of the weak hadronic decays of a heavy quark. Much of the data has come from the D-pair production results of the MARK II and MARK III detectors with recent and future additions anticipated from the Fermilab photoproduction experiment E691.[43] The establishment of the existence of some rare $D^0$ and $D^+$ decay modes has come from higher energy $e^+e^-$ storage ring data (DORIS and CESR) where despite larger backgrounds, the detection efficiencies can be higher. For similar reasons, the first observations of the $D_s$ (at ~ 1970 MeV/c$^2$) also came from the higher energy machines(CESR and PEP), and only recently are being augmented by data from the machines like SPEAR, running near $D_s\bar{D}_s$ production threshold. The data on hadronic weak decays is first reviewed here, and then in the final sections is discussed in light of the phenomenology of weak decays.

4.3.1 Cabibbo-allowed $D^0$ and $D^+$ decays. Table V summarizes the Cabibbo-allowed decays of the $D^0$ and $D^+$ with their production cross section times branching ratio ($\sigma \cdot B$) at the $\psi(3770)$ from the major experiments.[44][45][46][47][48]

TABLE V. Cabibbo-Allowed Decays of D Mesons
$\sigma \cdot Br$(nb) at $\sqrt(s) = 3.77$ GeV

| Decay Channel | MARK III[46,47,48] | MARK II[45] | LGW[44] |
|---|---|---|---|
| $D^0 \rightarrow$ | | | |
| $K^-\pi^+$ | $0.25 \pm 0.01 \pm 0.01$ | $0.24 \pm 0.02$ | $0.25 \pm 0.05$ |
| $\bar{K}^0\pi^0$ | $0.11 \pm 0.02 \pm 0.01$ | $0.18 \pm 0.08$ | - |
| $\bar{K}^0\eta$ | $0.09 \pm 0.04 \pm 0.01$ | - | - |
| $\bar{K}^0\omega$ | $0.19 \pm 0.07 \pm 0.05$ | - | - |
| $\bar{K}^0\phi$ | $0.05^{+0.03+0.02}_{-0.02-0.01}$ | - | - |
| $K^-\pi^+\pi^0$ | $0.76 \pm 0.04 \pm 0.08$ | $0.68 \pm 0.23$ | $1.4 \pm 0.6$ |
| $\bar{K}^0\pi^+\pi^-$ | $0.37 \pm 0.03 \pm 0.03$ | $0.30 \pm 0.08$ | $0.46 \pm 0.12$ |
| $\bar{K}^0K^+K^-$ | $0.05^{+0.02+0.01}_{-0.01-0.01}$ | - | - |
| $K^-\pi^+\pi^+\pi^-$ | $0.53 \pm 0.03 \pm 0.05$ | $0.68 \pm 0.11$ | $0.36 \pm 0.11$ |
| $\bar{K}^0\pi^+\pi^-\pi^0$ | $0.67 \pm 0.11 \pm 0.15$ | - | - |
| $D^+ \rightarrow$ | | | |
| $\bar{K}^0\pi^+$ | $0.14 \pm 0.01 \pm 0.01$ | $0.14 \pm 0.03$ | $0.14 \pm 0.05$ |
| $K^-\pi^+\pi^+$ | $0.39 \pm 0.01 \pm 0.03$ | $0.38 \pm 0.05$ | $0.36 \pm 0.06$ |
| $\bar{K}^0\pi^+\pi^0$ | $0.42 \pm 0.08 \pm 0.08$ | $0.78 \pm 0.48$ | - |
| $\bar{K}^0\pi^+\pi^+\pi^-$ | $0.31 \pm 0.03 \pm 0.03$ | $0.51 \pm 0.18$ | - |
| $K^-\pi^+\pi^+\pi^0$ | $0.18 \pm 0.04 \pm 0.04$ | - | - |
| $K^-\pi^+\pi^+\pi^-\pi^+$ | - | $\leq 0.23$ at 90% CL | - |

The principle decay modes of Table V are shown in Figure 14[15] and Figure 15.[46] The use of kinematic constraints at the $\psi(3770)$ allows mass resolutions comparable to the energy spread of the beam in the machine (typically 1.5 to 2 MeV/c$^2$). At higher energies, typical mass resolutions are 10 to 20 MeV/c$^2$, but as previously noted, detection efficiencies may be higher due to the significantly larger momenta which reduces the problem of strange particle decays. Figure 16 shows the W-exchange candidate $D^0 \to \bar{K}^0\phi$, first observed at higher energies,[49] while Figure 17 shows the isolation of this channel at the $\psi(3770)$.

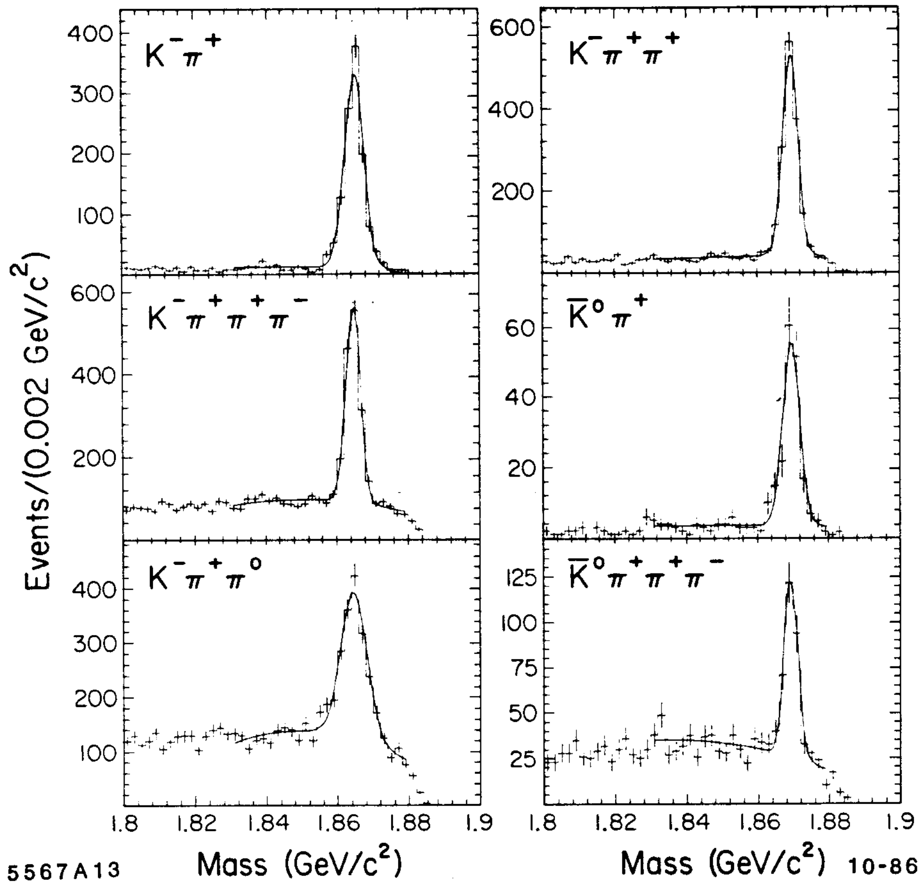


**Fig. 14. Examples of hadronic decays of $D^0$ and $D^+$ modes, using the beam constraint to improve mass resolution.**[15]

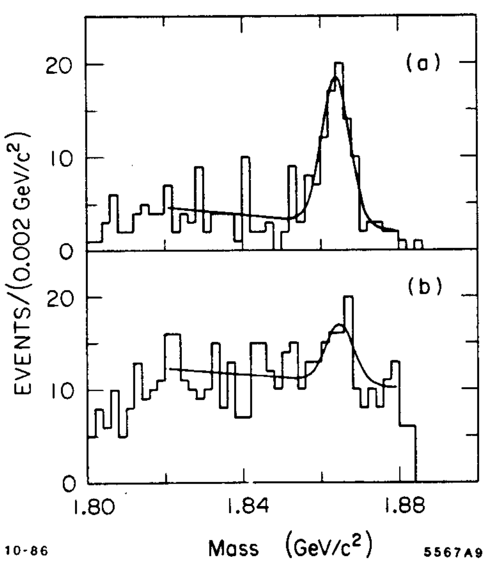


Fig. 15. The decays (a) $\bar{K}^0\pi^0$ and (b) $\bar{K}^0\eta$.[46]

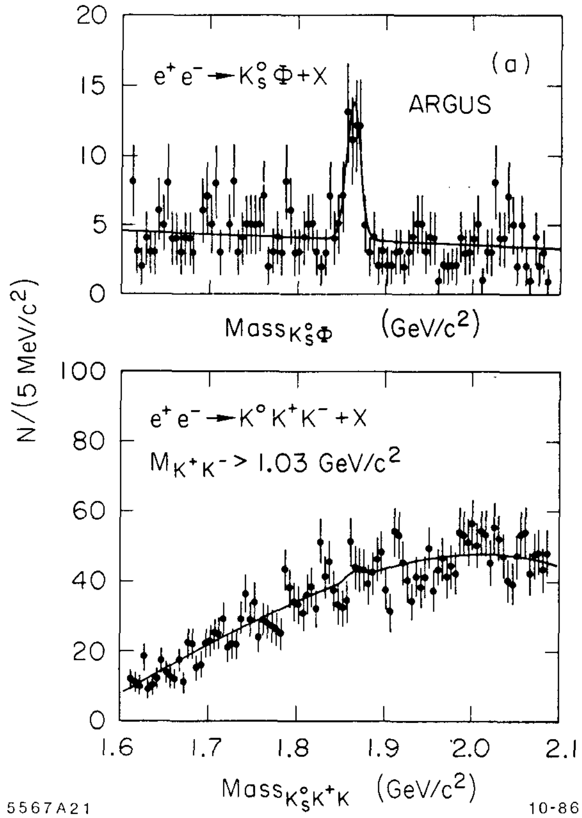


Fig. 16. The decay (a) $D^0 \to \bar{K}^0\phi$, and (b) $\bar{K}^0K^+K^-$ from high energy $e^+e^-$ data.[49]

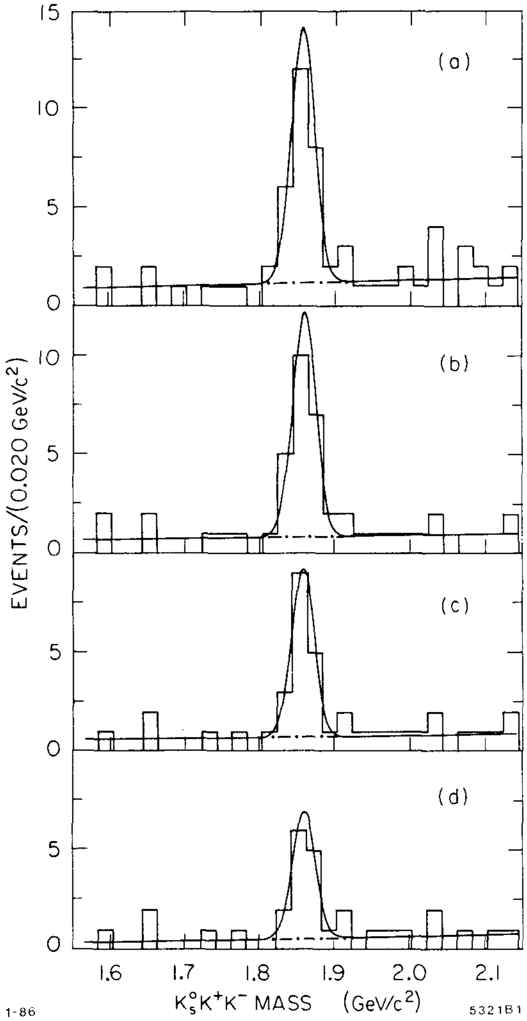


Fig. 17. $K^0_SK^+K^-$ events with successively tighter cuts on the decay angular distribution to isolate the $K^0_S\phi$ channel.[48]

4.3.2 Pseudoscalar-vector decays. Table V contains several large decay modes for 3- and 4-body final states. These modes are generally expected to contain resonant substructure in a ratio one would naively expect to be similar to the semileptonic $D_{l3}$ and $D_{l4}$ decays. Preliminary results on the breakdown of many three-body modes into quasi-two-body modes have only recently become available[50] and provide considerably more precise numbers than had been previously known.[45][51] Figure 18 shows an example of the quality of current data used to establish the resonant composition of the three-body decays. Table VI summarizes the pseudoscalar-vector content of the three-body decay modes.[50][47]

Almost no detailed information exists at the present time on the resonant substructure of the four-body decays, although there is evidence for the presence of underlying vector-vector decays.[52] Results are forthcoming from the MARK III and E691 experiments. Such information would be valuable since as shown in Table VI, it appears that a large fraction of the three-body decays are quasi-two-body. If the trend were to continue, a clear calculational simplification would result.

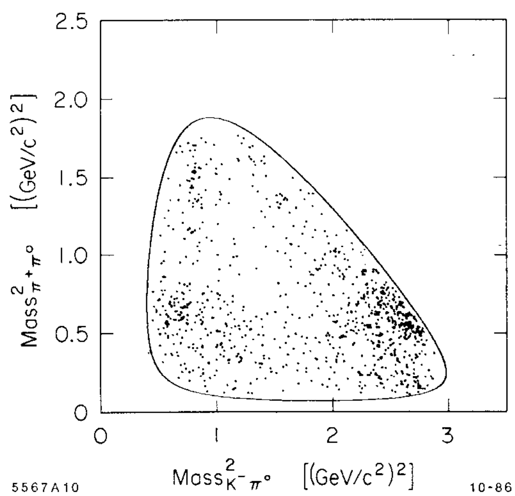


Fig. 18. The Dalitz plot for $D^0 \to K^-\pi^+\pi^0$.[50]

4.3.3 Branching ratios of charmed mesons. The decays of the $D^0$ and $D^+$ have thus far been given only in terms of their production rates ($\sigma \cdot Br$). This is advantageous for most theoretical comparisons, as it minimizes experimental errors, and avoids the uncertainty of absolute normalization. The overall scale of D meson branching ratios has been measured using two techniques. The traditional technique is to measure the height of the $\psi(3770)$ resonance over the continuum background by performing an energy scan and fit to the resonance. Since the $\psi(3770)$ is just above $D\bar{D}$ threshold and below $D\bar{D}^*$ threshold and since its total width is large (~25 MeV/c$^2$) compared to the nearby $\psi(3685)$, it is assumed to decay strongly into pairs of $D^0$ and $D^+$ . The height of the resonance gives the cross section for charm production with $D^0$ and $D^+$ produced in the phase-space ratio of about 55:45. The measurements vary however over a large range - from $11.5 \pm 2.5$ nb[53] to $6.8 \pm 1.2$ nb[54] - for the $D^0$ production cross section.[55]

A more recent measurement has been performed[47][56] which compares the number of fully reconstructed $D\bar{D}$ events at the $\psi(3770)$ to the number of single $D$ mesons observed, and which yields an even smaller cross section of $4.5\pm0.5$ nb for $D^0$ production. The general agreement in production rates between experiments (see Table V) suggests the possibility that the assumptions used in the resonance height calculation may be incorrect: in particular, that the $\psi(3770)$ may decay significantly to other final states. Radiative decays to other charmonium levels are expected to be a small part of the total width (a few hundred KeV).[57] It has been proposed that two-step OZI-allowed decays may provide a means for charmless OZI-forbidden decays to occur at threshold.[58] At present, the only measurement of $D\bar{D}$ production at the $\psi(3770)$ finds 1.09±0.23 $D\bar{D}$ for each $\psi(3770)$ decay.[59] By taking the average of the two most precise measurements of the cross section (6.8 nb and 4.5 nb), one is left with a residual uncertainty of about ±25% in the overall scale of D meson branching fractions.

TABLE VI. Pseudoscalar-Vector Content of the Three-body Cabibbo-Allowed Modes
$\sigma \cdot Br$(nb) at $\sqrt(s) = 3.77$ GeV[50] [47]

| Channel | Fraction(%) | $\sigma \cdot$Br(nb) |
|---|---|---|
| $D^0 \to K^-\pi^+\pi^0$ | | |
| $K^-\rho^+$ | $74.0 \pm 4.6 \pm 5.0$ | $0.56 \pm 0.05 \pm 0.07$ |
| $K^{*-}\pi^+$ | $12.9 \pm 2.7 \pm 2.0$ | $0.30 \pm 0.06 \pm 0.06$ |
| $\bar{K}^{*0}\pi^0$ | $7.6 \pm 3.3 \pm 2.0$ | $0.09 \pm 0.04 \pm 0.03$ |
| nonresonant | $5.5 \pm 4.4 \pm 3.0$ | $0.04 \pm 0.03 \pm 0.02$ |
| $D^0 \to \bar{K}^0\pi^+\pi^-$ | | |
| $\bar{K}^0\rho^0$ | $16.8 \pm 5.3 \pm 2.5$ | $0.06 \pm 0.02 \pm 0.01$ |
| $K^{*-}\pi^+$ | $63.9 \pm 7.6 \pm 4.5$ | $0.36 \pm 0.05 \pm 0.04$ |
| nonresonant | $19.3 \pm 8.6 \pm 3.5$ | $0.07 \pm 0.03 \pm 0.01$ |
| $D^+ \to \bar{K}^0\pi^+\pi^0$ | | |
| $\bar{K}^0\rho^+$ | $86.5 \pm 9.1 \pm 5.0$ | $0.37 \pm 0.08 \pm 0.07$ |
| $K^{*0}\pi^+$ | $7.0 \pm 4.3 \pm 4.0$ | $0.09 \pm 0.06 \pm 0.06$ |
| nonresonant | $6.5 \pm 5.5 \pm 4.0$ | $0.03 \pm 0.02 \pm 0.02$ |

4.3.4 Cabibbo-suppressed D meson decays. Table VII lists various measurements of Cabibbo-suppressed decays of the $D^0$ and $D^+$.[48] [60] [61]

Figure 19 and Figure 20 show the capability of current data to inclusively separate typical two-body Cabibbo-suppressed decays.[60] The second peaks are reflections of cabibbo-allowed decays where particle misidentification has occurred. Figure 21 shows two- three- and four-body Cabibbo-suppressed decays containing neutral pions, cleanly isolated by requiring fully reconstructed $D\bar{D}$ events at the $\psi(3770)$.

TABLE VII. Cabibbo-Suppressed Decays of D Mesons
Relative Rates and Br(%)

| Decay Channel | Ratio |
|---|---|
| $D^0$ Decays | |
| $\frac{\Gamma(\pi^-\pi^+)}{\Gamma(K^-\pi^+)}$ | $0.033 \pm 0.010 \pm 0.006$ |
| $\frac{\Gamma(K^-K^+)}{\Gamma(K^-\pi^+)}$ | $0.122 \pm 0.018 \pm 0.012$ |
| $\frac{\Gamma(\bar{K}^0K^0)}{\Gamma(K^-\pi^+)}$ | $\leq 0.11$ *at* 90% *C.L.* |
| $\frac{\Gamma(\bar{K}^{*0}K^0+cc)}{\Gamma(K^{*-}\pi^+)+\Gamma(K^-\rho^+)}$ | $\leq 0.034$ *at* 90% *C.L.* |
| $\frac{\Gamma(\bar{K}^{*-}K^++cc)}{\Gamma(K^{*-}\pi^+)+\Gamma(K^-\rho^+)}$ | $0.05 \pm 0.03$ |
| $\frac{\Gamma(\pi^-\pi^+\pi^0)}{\Gamma(D^0\rightarrow all)}$ | $0.011 \pm 0.004 \pm 0.002$ |
| $\frac{\Gamma(\pi^-\pi^+\pi^+\pi^-)}{\Gamma(D^0\rightarrow all)}$ | $0.015 \pm 0.006 \pm 0.002$ |
| $D^+$ Decays | |
| $\frac{\Gamma(\bar{K}^0K^+)}{\Gamma(\bar{K}^0\pi^+)}$ | $0.317 \pm 0.086 \pm 0.048$ |
| $\frac{\Gamma(\pi^+\pi^0)}{\Gamma(\bar{K}^0\pi^+)}$ | $\leq 0.15$ *at* 90%*C.L.* |
| $\frac{\Gamma(\pi^-\pi^+\pi^+)}{\Gamma(K^-\pi^+\pi^+)}$ | $0.042 \pm 0.016 \pm 0.010$ |
| $\frac{\Gamma(K^-K^+\pi^+)}{\Gamma(K^-\pi^+\pi^+)}$ | $0.059 \pm 0.026 \pm 0.009$ |
| $\frac{\Gamma(\phi\pi^+)}{\Gamma(K^-\pi^+\pi^+)}$ | $0.084 \pm 0.021 \pm 0.011$ |
| $\frac{\Gamma(K^{*0}K^+)}{\Gamma(K^-\pi^+\pi^+)}$ | $0.048 \pm 0.021 \pm 0.011$ |

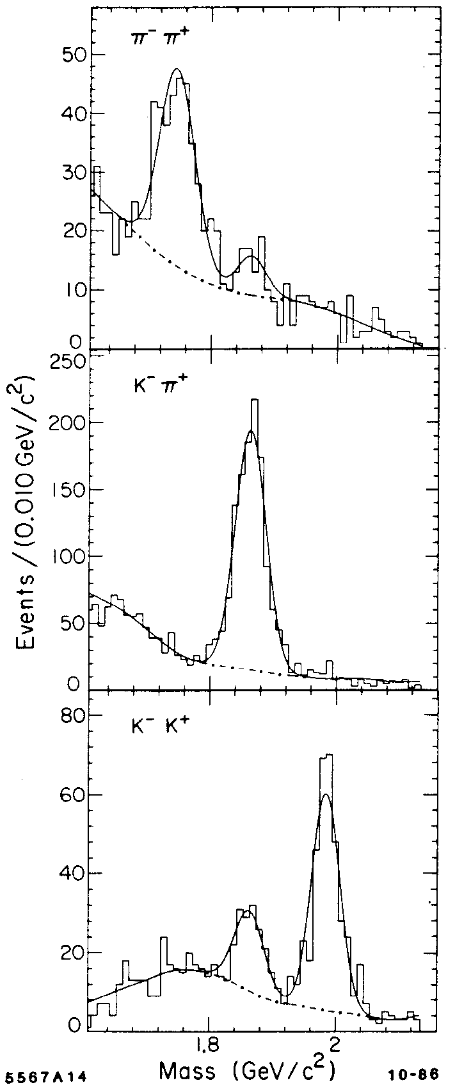


Fig. 19. The decays $D^0 \to K^+K^-$, $K^-\pi^+$, and $\pi^+\pi^-$.[60]

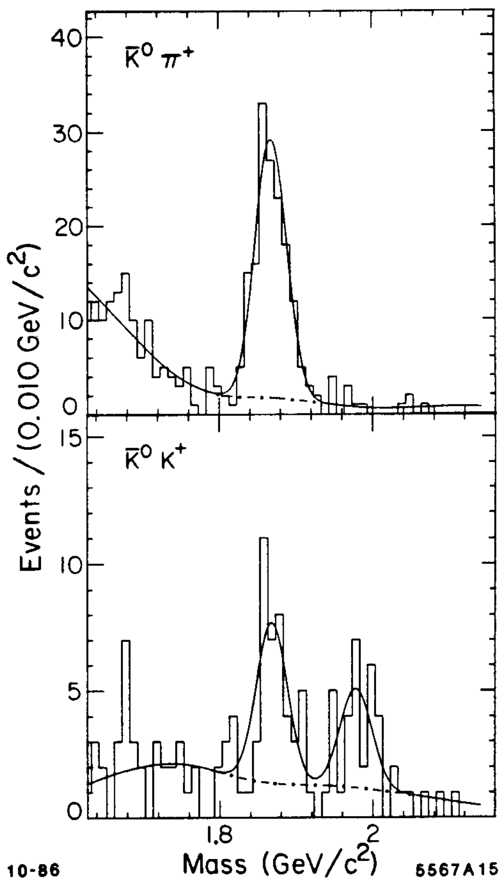


Fig. 20. The decays $D^+ \to \bar{K}^0 K^+$ and $\bar{K}^0\pi^+$.[60]

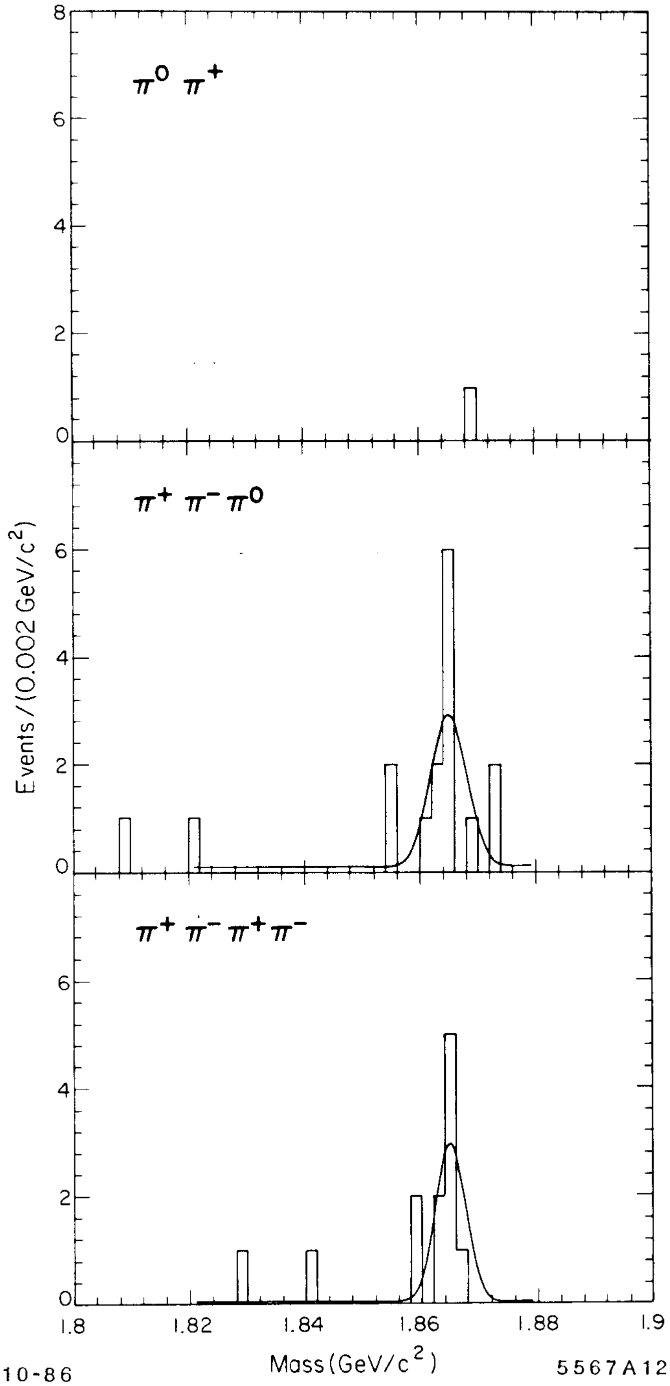


Fig. 21. Rare Cabibbo-suppressed decays isolated opposite tagged $D^0$ and $D^+$.[60]

4.3.5 The $D_s$ hadronic decays. In Table VIII are listed the observed decays of the $D_s$ from both hadroproduction and $e^+e^-$ experiments.[43] [62] [63]

Figure 22 shows the clean isolation of the $D_s$ from low energy $e^+e^-$ associated $(D\bar{D}^*)$ production. As yet, no experiment can directly measure the absolute branching ratios for the $D_s$ meson. By scaling the well known $\mu$-pair cross section well above $D_s\bar{D}_s$ threshold by 3 (color)$\times$0.15 ($s\bar{s}$ extraction from the vacuum)$\times(\frac{2}{3})^2$ (c-quark charge), the higher energy experiments obtain Br($D_s \rightarrow \phi\pi^+$) $\approx$ 4%. There is no reason that these assumptions would be valid in the lower energy data, which is close to thresholds. However, with a large increase in data, the double tag technique[47] as used for $D^0$ and $D^+$ would be available at the lower energies where $D_s$ pair or associated production is occurring, thus enabling the assumption-free extraction of absolute branching ratios for one or more decay modes.

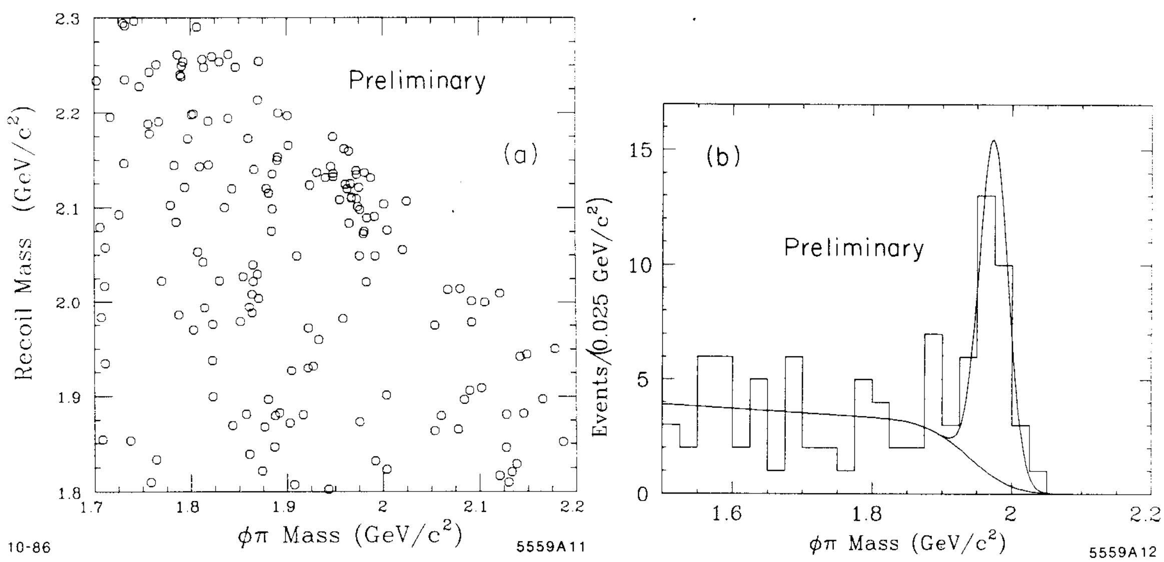


Fig. 22. Preliminary results for $D_s \rightarrow \phi\pi^+$ from $D_s\bar{D}_s^*$ associated production at SPEAR.[63] The recoil mass distribution (a) is cut between 2.04 and 2.18 GeV/c$^2$ to produce the $D_s$ signal in (b).

TABLE VIII. Decays of the $D_s$ Mesons[7] [43] [62] [63]
((†) indicates a preliminary result)

| Experiment | $\sqrt{(s)}$ (GeV) | Beam | Channel | Mass (MeV/c$^2$) |
|---|---|---|---|---|
| CLEO | 10 | $e^+e^-$ | $\phi\pi^+$ | $1970 \pm 5 \pm 5$ |
| TASSO | 14-25 | $e^+e^-$ | $\phi\pi^+$ | $1975 \pm 9 \pm 10$ |
| ARGUS | 10 | $e^+e^-$ | $\phi\pi^+$ | $1973 \pm 3 \pm 3$ |
| ARGUS | 10 | $e^+e^-$ | $\phi\pi^+\pi^-\pi^+$ | $1976 \pm 5 \pm 3$ |
| TPC | 29 | $e^+e^-$ | $K^-K^+\pi^+$ | $1948 \pm 28 \pm 10$ |
| HRS | 29 | $e^+e^-$ | $\phi\pi^+$ | $1963 \pm 3 \pm 3$ |
| ACCMOR | 200 | $(\pi, N), (K, N)$ | $K^-K^+\pi^+$ | $1975 \pm 4$ |
| ARGUS | 10 | $e^+e^-$ | $\bar{K}^{*0}K^+$ | *seen* |
| MARK III | 4.14 | $e^+e^-$ | $\phi\pi^+$ | $1973 \pm 4 \pm 4^{\dagger}$ |
| MARK III | 4.14 | $e^+e^-$ | $\bar{K}^{*0}K^+$ | *seen* |
| MARK III | 4.14 | $e^+e^-$ | $\bar{K}^0K^+$ | *seen* |
| TPS | 260 | $\gamma N$ | $\phi\pi^+$ | *seen* |
| TPS | 260 | $\gamma N$ | $\bar{K}^{*0}K^+$ | *seen* |

### 4.4 Experimental Results on $D^0\bar{D}^0$ Mixing

As discussed in Section 3.2.4, r for $D^0\bar{D}^0$ mixing may be as large as a few $\times 10^{-3}$. Two experimental avenues for measuring mixing have been explored. In the first, charmed pairs are produced through hadro[64] [65] - or neutrino-production[66] or muon-scattering[67] and mixing is studied through the events wherein both charmed mesons decay semileptonically. The mixing signature is events containing like-sign lepton pairs. These experiments are often forced to make assumptions about the charm cross section and the precise production mechanism. The second method is to *tag* charm either through the cascade $D^{*+} \to \pi^+ D^0$ or through $D\bar{D}$ pair-production and the reconstruction of both of the charmed mesons. The second method has been used in photoproduction[68] and $e^+e^-$ production of charm.[5] [7] [69] [70] [71] [72] [73] Table IX summarizes the current data.

TABLE IX. Limits on $D^0\bar{D}^0$ Mixing
((†) indicates a preliminary result)

| Reaction | Signature | Limit at 90% C.L. |
|---|---|---|
| $e^+e^-$ [5] | $\frac{D^0 \to K^+X}{\bar{D}^0 \to K^-X}$ | $r < 0.18$ |
| $e^+e^-$ [69] | $D^{*+} \to \pi^+ D^0$ | $r < 0.16$ |
| $\gamma N$ [68] | $D^{*+} \to \pi^+ D^0$ | $r < 0.11$ |
| $(\pi, p)N$ [64] | $\frac{N(\mu^\mp\mu^\mp)}{N(\mu^+\mu^-)}$ | $r < 0.44$ |
| $e^+e^-$ [70] | $D^{*+} \to \pi^+ D^0$ | $r < 0.081$ |
| $\mu N$ [67] | $\frac{\mu^\mp N \to \mu^\mp\mu^\pm\mu^\pm}{\mu^\mp N \to \mu^\mp\mu^+\mu^-}$ | $r < 0.012$ |
| $\pi N$ [65] | $\frac{N(\mu^\mp\mu^\mp)}{N(\mu^+\mu^-)}$ | $r < 0.0056$ |
| $\nu N, \bar{\nu} N$ [66] | $\frac{N(\mu^\mp\mu^\mp)}{N(\mu^+\mu^-)}$ | $r_{\bar{\nu}} = 0.03, r_\nu = 0.05$ |
| $e^+e^-$ [71] | $D^{*+} \to \pi^+ D^0$ | $r < 0.023$ |
| $e^+e^-$ [72] | $D^{*+} \to \pi^+ D^0$ | $r < 0.040$ |
| $e^+e^-$ [7] [73] | $D^0\bar{D}^0$ reconstructed | $r \sim 0.01^\dagger$ |

While the hadroproduction result of ref.[65] has produced the most stringent limit, it requires a large subtraction and understanding of the charm production process. The less model dependent *tag* measurements are now sensitive to r≈ 0.01. An intriguing result from the MARK III experiment[73] is shown in Figure 23. Three events are found with total strangeness ($s$) of ±2, in a sample of 162 ordinary $s = 0$ events. The expected background from particle misidentification is ~ 0.4 events. These events could arise however from doubly Cabibbo suppressed decays, since they come from two $D^0$ in nonidentical final states.[74] To improve mixing limits beyond this requires understanding the doubly suppressed component. Another possibility is to work at several decay lengths from the production vertex to enhance the mixing component over the doubly Cabibbo-suppressed component. This may be possible in the near future, with the steady improvement of electronic vertexing techniques.

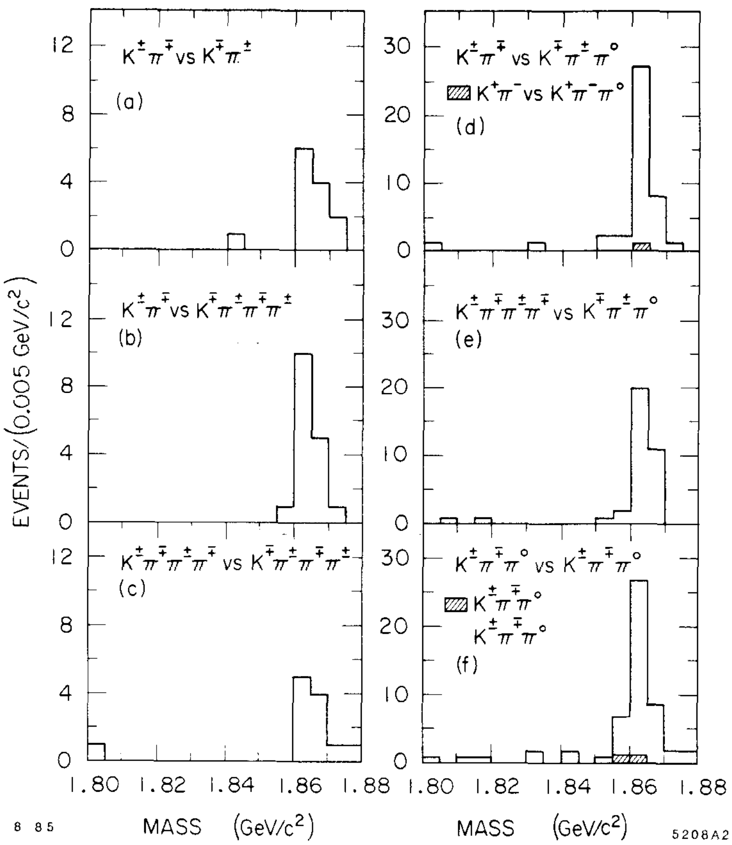


Fig. 23. Fully reconstructed $D^0\bar{D}^0$ events showing three candidate mixing events.[73]

## 5. INTERPRETATION OF DATA ON WEAK HADRONIC DECAYS

The following sections discuss the present data in terms of the theory and phenomenology presented in Section 3. Emphasis is placed on the enumeration of evidence for each of the important concepts. The final section attempts to coherently bring these ideas together.

## 5.1 Color Suppression

The first and simplest tests of the theoretical ideas of Section 3.2.3 concern the well measured values of the color-suppressed to non-suppressed decay widths:[46] [60] [63]

$$\frac{\Gamma(D^0 \to \bar{K}^0\pi^0)}{\Gamma(D^0 \to K^-\pi^+)} = 0.45 \pm 0.08 \pm 0.05$$

$$\frac{\Gamma(D^0 \to \bar{K}^{*0}\pi^0)}{\Gamma(D^0 \to K^{*-}\pi^+)} = 0.29 \pm 0.14 \pm 0.09$$

$$\frac{\Gamma(D^0 \to \bar{K}^0\rho^0)}{\Gamma(D^0 \to K^-\rho^+)} = 0.11 \pm 0.04 \pm 0.02$$

$$\frac{\Gamma(D^+ \to \phi\pi^+)}{\Gamma(D^+ \to K^-\pi^+\pi^+)} = 0.08 \pm 0.02 \pm 0.01$$

$$\frac{\Gamma(D_s^+ \to \bar{K}_s^0 K^+)}{\Gamma(D_s^+ \to \phi\pi^+)} = 0.44 \pm 0.12 \pm 0.21$$

In no instance is a significant suppression observed for color mismatched decays. It has been argued that final state interactions may play a significant role in D decays.[75] However, in *all* cases, the suppression expected from the naive spectator model is absent. In particular, this appears to be true for *both* $D^0$ and $D^+$ decays. The naive interpretation is the presence of soft (non-perturbative) gluons in the meson which lift the precise color matching required by the perturbative calculations. Calculationally, the effect is introduced by the *screening factor*($\xi$) discussed in Section 3.2.3, which largely removes these cancellations. It should be noted once again that the need to introduce the parameter $\xi \approx 0$ to get the weak hadronic decays correct also reduces $B_l$ for the $D^0$ (see eqn. 5), further improving the agreement with the measurements.

## 5.2 Weak Flavor-Annihilation and Non-Spectator Decays

The search for direct evidence for W-exchange graphs in $D^0$ decays can be summarized by the following results:

$$Br(D^0 \to \bar{K}^0\phi) \approx 1.5\%$$

$$\frac{\Gamma(D^0 \to \bar{K}^0 K^0)}{\Gamma(D^0 \to K^-\pi^+)} \leq 0.11 \text{ at } 90\% C.L.$$

$$\frac{\Gamma(\bar{K}^{*0} K^0 + cc)}{\Gamma(K^{*-}\pi^+) + \Gamma(K^-\rho^+)} \leq 0.034 \text{ at } 90\%\ C.L.$$

The first channel, $D^0 \to \bar{K}^0\phi$, is clearly seen by three experiments,[76][48] although the precise branching ratio differs between experiments due to their assumptions of the backgrounds. This channel is Cabibbo-allowed and surprisingly occurs at a rate which is consistent with that for *ordinary* pseudoscalar-vector decays after a reduction for the limited phase-space and a factor for the removal of an $s\bar{s}$ pair from the vacuum is taken into account.[22][76] This suggests that if W-exchange is present, it is proceeding at a rate which is largely uninhibited. The same non-perturbative gluon effects suspected for the absence of color cancellations, may also lift the helicity suppression of this channel. Alternately, as pointed out in Section 3.2.1, this decay may arise from rescattering effects and not from the W-exchange mechanism itself. The second decay ($D^0 \to \bar{K}^0 K^0$) is Cabibbo-suppressed and is suppressed in exact SU(3). The limit is already below the value measured for the $K^+K^-$ decay (see Table VII), but it is not stringent enough to give additional information. The third channel ($D^0 \to \bar{K}^{*0}K^0$) is Cabibbo-suppressed but not SU(3)-suppressed. While the value of the limit is preliminary,[61] it is *intriguingly* small considering the size of Br($D^0 \to \bar{K}^0\phi$). Future measurements in the D meson sector that would clarify the W-exchange issue will likely deal with these three decay modes.

None of the current $D_s$ measurements of Table VIII provides unique information on the presence of W-annihilation graphs, as they all may arise from spectator amplitudes. Only measurements such as $D_s \to \rho\pi, \omega\pi....$, will answer the question of W-exchange and W-annihilation, as would inclusive measurements of $D_s$ decays opposite *tagged* $D_s$ .

### 5.3 Interference Effects in $D^+$ Decays

Evidence for interference (Section 3.2.2) in exclusive decays comes from the following comparisons:

$$\frac{\Gamma(D^+ \to \bar{K}^0 K^+)}{\Gamma(D^0 \to \bar{K}^0 \pi^+)} = 0.32 \pm 0.09 \pm 0.05 \tag{7}$$

$$\frac{\Gamma(D^+ \to \pi^+ \pi^0)}{\Gamma(D^0 \to \bar{K}^0 \pi^+)} \leq 0.15 \text{ at } 90\% \; C.L. \tag{8}$$

$$\frac{\Gamma(D^+ \to \bar{K}^{*0} K^+)}{\Gamma(D^0 \to \bar{K}^{*0} \pi^+)} = 0.21 \pm 0.17 \pm 0.15 \tag{9}$$

As can be seen from Figure 8, interference effects are expected for both $\pi^+\pi^0$ and $\bar{K}^0\pi^+$, but not for $\bar{K}^0 K^+$ or $\bar{K}^{*0}K^+$. Thus, since each of the numerators in (7) and (9) is Cabibbo-suppressed, one expects values close to $tan^2(\theta_c) \approx 0.055$ for the ratios. Expression (8) however, is expected[40] to be given by $\frac{1}{2}tan^2(\theta_c)$ although as pointed out earlier, SU(3)-breaking and final-state interactions may alter the value.[26] The deviation from equality in partial widths expected under exact SU(3) for the well measured Cabibbo-suppressed decays $D^0 \to \pi^+\pi^-$ and $D^0 \to K^+K^-$ (see Table VII) sets the scale for the size of these effects in charm decay.[77] While (8) is clearly consistent with expectations, (7) and (9) are considerably larger, even including the possibility of large SU(3)-violations or final-state interactions. This is then entirely consistent with the pattern expected for interference among $D^+$ final state amplitudes, which may lead to a longer $D^+$ lifetime.

### 5.4 Summary of the Hadronic Decays

In summary, the two-body weak-hadronic decays of ground state charmed mesons ($D^o$,$D^+$ and $D_s$ ) rule out the exact color suppression mechanism originally anticipated. The origin of its absence may lie with the presence of soft gluons introducing non-perturbative effects. The differences in lifetimes between the charmed mesons may indirectly arise from this source. The presence of additional gluons may act to catalyze specific mechanisms such as W-exchange and W-annihilation, shortening the $D^0$ and $D_s$ lifetimes. At least one mechanism - gluon radiation - can be largely ruled out from recent measurements,[7] while one of a non-perturbative origin - gluons in the meson wavefunction - cannot.[26] Evidence for at least one candidate exclusive channel exists, ($D^0 \rightarrow K^0\phi$), although the possibility of its creation through strong interaction rescattering (rather than W-exchange) cannot be ruled out.[23][24] Experiments are not yet sensitive to other W-exchange channels. Interference effects lengthening the $D^+$ lifetime appear to be present as evidenced from the pattern of the exclusive decays of the $D^+$ (see eqns. (7)-(9)).

The sum of all the measured channels for the $D^0$ and $D^+$ from Tables III,V,VI, and VII, using the normalization of refs.[47,56], implies that about 80% of all D decays are accounted for. As is evident, a large fraction of the decays are quasi-two-body, being pseudoscalar-pseudoscalar, and pseudoscalar-vector. If the higher multiplicity decays are largely vector-vector and the balance of the unseen decays follow the same pattern, then the prescription of refs.[24,32] for calculating exclusive decays can be applied. By summing over all channels, it would appear that the non-leptonic widths of the $D^0$ and the $D^+$ should differ by a factor of 2 to 3, which could roughly account for the observed lifetimes. This result is remarkable in its simplicity, since the origin of the difference is largely accounted for by $D^+$ interference. Phase shifts from final state interactions and form-factors are only simply incorporated, while W-exchange is ignored. Alternative approaches applying QCD corrections (without the screening factor), factorization of matrix elements, and a large W-annihilation component, have also produced reasonable agreement with data.[78] It is clear that a critical test will be the accurate prediction of the pattern of $D_s$ decays, wherein the role of W-annihilation may be significant.[79]

## 6. CONCLUSIONS

The investigation of charmed mesons has progressed rapidly since their discovery in the mid 1970's. The spectroscopy of the $c\bar{q}$ system is only now being tested by the modern and more sensitive detectors at higher energies. The decays of the charm system provide a unique laboratory in which to study the subtle interplay of the strong and weak interactions. Unlike in the case of the lighter mesons, the study of charm is facilitated by the enormous simplification due to the onset of asymptotic freedom. Yet, it still suffers in detail, as does the slightly heavier beauty system, from the complications that arise from the residual - logarithmically falling - strong interaction. The modern data samples are sensitive to the effects, making the understanding of charm both a theoretical challenge and a real prerequisite to the true understanding of the heavier quark systems. Experiment and theory have clearly come a long way down the road towards understanding both the spectroscopy and the decays of charmed particles. The next few years should provide answers to the few remaining questions.

1. Gaillard, M. Lee, B. and Rosner, J., Rev. Mod. Phys. 47, 277 (1975).

2. Aguilar-Benitez, M. *et al.*, Phys. Lett. 170B, 1 (1986).

3. Lüth, V., Proceedings of the International Symposium on Production and Decay of Heavy Flavors,Heidelberg, May 20-23 (1986).

4. Abachi, S. *et al.*, Preprint ANL-HEP-CP-86-50 June (1986).

5. Goldhaber, G. *et al.*, Phys. Lett. 69B, 503 (1977),
Feldman, G. *et al.*, Phys. Rev. Lett. 38, 1313 (1977).

6. Aihara, H. *et al.*, Phys. Rev. Lett. 53, 2465 (1984),
Albrecht, H. *et al.*, Phys. Lett. 146B, 111 (1984),
Asratyan, A.E. *et al.*, Phys. Lett. 156B, 441 (1985).

7. Schindler, R.H., Proceedings of the XXIII International Conference on High Energy Physics, Berkeley, California, July 16-23 (1986). SLAC-PUB-4055.

8. See for example; De Rujula, A. *et al.*, Phys. Rev. D12, 143 (1975).
De Rujula, A. *et al.*, Phys. Rev. Lett. 37, 398 (1976).
Eichten, E. *et al.*, Phys. Rev. D21,203 (1980).
Godfrey, S. and Isgur, N., Phys. Rev. D32,189 (1985).

9. Albrecht, H. *et al.*, Phys. Rev. Lett. 56, 549 (1986),
Evidence also appears in Goldhaber, G. *et al.*, Phys. Lett. 69B, 503(1977).

10. $B^*$ mass from Han, K. *et al.*, Phys. Rev. Lett. 55, 36 (1986), and assuming an average B mass of $5277 \pm 4$ MeV/c$^2$.

11. Frank, M. and O'Donnell, P., Phys. Lett. 159B, 174 (1985),
Igi, K. and Ono, S., Phys. Rev. D32, 232 (1985).

12. For an excellent review see Rückl, R., "Weak Decays of Heavy Flavours," Habilitationschrift Univ. München, CERN-PRINT (1983), and references therein.

13. Altarelli, G. *et al.*, Phys. Lett. 99B, 141 (1981).

14. Igarashi, Y., Kitakado, S., and Kuroda, M., Phys. Lett. 93B, 125 (1980),
Deshpande, N., Gronau, M., and Sutherland, D., Phys.Lett 90B,431 (1980),

Gronau, M. and Sutherland, D., Nucl. Phys. B183, 367 (1981).

15. Baltrusaitis, R.M. *et al.*, Phys. Rev. Lett. 54, 1976 (1985)

16. Schindler, R.H. *et al.*, Phys. Rev. D24, 78 (1981),
Bacino, W. *et al.*, Phys. Rev. Lett. 45, 329 (1980).

17. Rosen, S.P., Phys. Rev. Lett. 44, 4 (1980).

18. Fritzsch, H. and Minkowski, P., Phys. Lett. 90B, 455 (1980).

19. Bander, M., Silverman, D. and Soni, A., Phys. Rev. Lett. 44, 7 (1980).

20. See for example: Sinha, S.N., U. of Alberta Preprint Thy-3-86 (1986),
O'Donnell, P.J., CERN-TH-4419/86 (1986),
Maiani, L., Proceedings of the XXI International Conference on High Energy Physics, (Editions de Physique, Le Ulis, France, 1982), pp. 631-657,
Krasemann, H., Phys. Lett. 96B, 397 (1980),
Mathur, V.S. and Yamawaki, M.T., Phys. Rev. D29, 2057 (1984),
Novikov, V.A. *et al.*, Phys. Rev. Lett. 38, 626 (1977).

21. Lusignoli, M. and Pugliese, A., INFN Roma Preprint-515 July (1986).
Hussain, F. and Kamal, A.N., U. of Alberta Preprint Thy-17-86 (1986).

22. Bigi, I.I.Y. and Fukugita, M., Phys. Lett. 91B, 121 (1980).

23. Donoghue, J.F., U. of Mass., Amherst, Preprint UMHEP-241(1986),
Hussain, F. and Kamal, A.N., U. of Alberta Preprint Thy-1-86,(1986).

24. Stech, B., "Perspectives in Electroweak Interactions and Unified Theories," XXIth Moriond Conference, ed. J.Tran Thanh Van, (1986).

25. Kamal, A.N., Phys. Rev. D33, 1344 (1986).

26. Bigi, I.I.Y., Proceedings of the 15th SLAC Summer Institute on Particle Physics, Stanford CA., July 28-August 5 (1986). SLAC-PUB-4067.

27. Interference was first proposed by Guberina, B., Peccei, R. and Rückl, R., Phys. Lett. 89B, 111 (1979).

28. Koide, Y., Phys.Rev. D20, 1739 (1979),
Bigi, I.I.Y., Z.Phys. C6, 83 (1980).

29. Kobayashi, T. and Yamazaki, Y., Prog. Theor. Phys. 65, 775 (1981).

30. Altarelli, G. and L.Maiani, L., Phys. Lett. 118B, 414 (1982),
Bilic, N. Guberina, B. and Trampetic, J., Nucl. Phys. B248, 261 (1984).

31. Ellis, J., Gaillard, M.K. and Nanopoulos, D.V., Nucl.Phys. B100, 313 (1976),
Cabibbo, N. and Maiani, L., Phys. Lett. 73B, 418 (1978),
Fakirov D. and Stech, B., Nucl. Phys. B133, 315 (1978).

32. Bauer, M. and Stech, B., Phys. Lett. 152B, 380 (1985),
Stech, B., "Flavor Mixing and CP Violation," 5th Moriond Workshop, ed. J.Tran Thanh Van, p.151(1985).

33. Buras, A.J., Gérard, J.M., and Rückl, R., Nucl.Phys. B268, 16 (1986).

34. Shifman, M.A., Voloshin, M.B., preprint ITEP-62(1984).

35. For an excellent review of $D^0\bar{D}^0$ mixing see Yamamoto, H., Ph.D.Thesis, California Institute of Technology, CALT-68-1318, pp 56-67 (1986), and references therein.

36. Gaillard, M. and Lee, B., Phys. Rev. D10, 897 (1986).

37. Wolfenstein, L., Phys. Lett. 164B, 170 (1985).

38. Aguilar-Benitez, M. *et al.*, Phys. Lett. 170B (1986).

39. Coffman, D.H., Proceedings of the XXIst Rencontre de Moriond, ed.J.Tran Thanh Van, March 9-16 (1986).

40. Chau, L.L.-, Phys. Rept. 95, 1 (1983).

41. Abramowicz, H. *et al.*, Z.Phys. C15, 19 (1982).

42. See Aguilar-Benitez, M. *et al.*, ref.[38], pp. 74-75 for a discussion.

43. Karchin, P., Proceedings of the XXIII International Conference on High Energy Physics, Berkeley, CA, July 16-23 (1986).

44. Peruzzi, I. *et al.*, Phys. Rev. Lett. 39, 1301 (1977),
Scharre, D. *et al.*, Phys. Rev. Lett. 40, 74 (1978)

45. Schindler, R.H. *et al.*, Phys. Rev. D24, 78 (1981).

46. Hauser, A.J., PhD Thesis, California Institute of Technology, unpublished (1984).

47. Baltrusaitis, R.M. *et al.*, Phys. Rev. Lett. 56, 2140 (1986).

48. Baltrusaitis, R.M. *et al.*, Phys. Rev. Lett., 56, 2136 (1986).

49. Albrecht, H. *et al.*, Phys. Lett. 158B, 525 (1985).

50. See for example, Schindler, R.H., Proceedings of the 14th SLAC Summer Institute on Particle Physics, Stanford, CA. July (1985).

51. Summers, D. *et al.*, Phys. Rev. Lett. 52, 410 (1984).

52. Piccolo, M. *et al.*, Phys. Lett. 70B, 260 (1977).

53. Peruzzi, I. *et al.*, Phys. Rev. Lett. 39, 1301 (1977).

54. Sadrozinski, H., High Energy Physics-1980, ed. Loyal Durand and Lee Pondrom, AIP Conference Proceedings No 68 (American Institute of Physics, New York, 1981), p681.

55. An intermediate value comes from Schindler, R.H *et al.*, Phys. Rev. D21, 2716 (1980).

56. For further details see Blaylock, G., Ph.D. Thesis, U. of Illinois (Urbana), unpublished (1986).

57. Lane, K., Harvard Preprint HUTP-86/A045, June (1986).

58. Lipkin, H., Argonne Preprint ANL-HEP-86-43.

59. Feller, J., Ph.D. Thesis, U. of Cal., Berkeley, LBL-9017-MC May (1979).

60. Baltrusaitis, R.M. *et al.*, Phys. Rev. Lett. 55, 150 (1985).

61. Baltrusaitis, R.M. *et al.*, SLAC-PUB-3858 December (1985).

62. Chen, C. *et al.*, Phys. Rev. Lett. 51, 634 (1983),
Aihara, H. *et al.*, Phys. Rev. Lett. 53, 2465 (1984),
Althoff, H. *et al.*, Phys. Lett. 136B, 130(1984),
Bailey, R. *et al.*, Phys. Lett. 139B, 320(1984),

Albrecht, H. *et al.*, Phys. Lett. 153B, 343(1985),
Derrick, M. *et al.*, Phys. Rev. Lett. 54, 2568 (1985).

63. Toki, W., Talk presented at the 15th SLAC Summer Institute on Particle Physics, July 28-August 8 (1986). These results are preliminary in nature.

64. Bodek, A. *et al.*, Phys. Lett. 113B, 82 (1982).

65. Louis, W.C. *et al.*, Phys. Rev. Lett. 56, 1027 (1985).

66. Burkhardt, H. *et al.*, Preprint CERN-EP 85-191.

67. Benvenuti, A. *et al.*, Phys. Lett. 158B, 531 (1985).

68. Avery, P. *et al.*, Phys. Rev. Lett. 44, 1309 (1980).

69. Feldman, G. *et al.*, Phys. Rev. Lett. 38, 1313 (1977).

70. Yamamoto, H. *et al.*, Phys. Rev. Lett. 54, 522 (1985).

71. ARGUS Collaboration, paper submitted to the the XXIII International Conference on High Energy Physics, Berkeley, California, July 16-23 (1986).

72. Abachi, S. *et al.*, preprint ANL-HEP-PR-86-100, July (1986).

73. Gladding, G.E., Talk presented at the 5th International Conference on Physics in Collision, Autun, France , July 2-5, (1985).

74. Bigi, I.I.Y. and Sanda, A., Phys. Lett. 171B, 320 (1986).

75. Lipkin, H., Phys. Rev. Lett. 44, 710 (1980).

76. Albrecht, H. *et al.*, Phys. Lett. 158 B,525 (1985),
Bebek, C. *et al.*, Phys. Rev. Lett. 56,1983(1986).

77. See Kamal, A.N. and Verma, R.C., U. of Alberta Preprint Thy-13-86 (1986), for a recent discussion of SU(3)-symmetry and final-state interactions in charm decays.

78. See for example, Hussain, F. and Kamal, A.N., ref.[21].

79. Kamal, A.N., and Sinha, S.N., U. of Alberta Preprint Thy-18-86 (1986).